Available online at www.sciencedirect.com
SCIENCE DIRECT®
Wave Motion 43 (2005) 29–50
WAVE MOTION
www.elsevier.com/locate/wavemoti

Embedded Rayleigh–Bloch surface waves along periodic rectangular arrays

R. Porter*, D.V. Evans

School of Mathematics, University of Bristol, Bristol BS8 1TW, UK

Received 6 July 2001; received in revised form 2 May 2005; accepted 23 May 2005
Available online 1 July 2005

Abstract

In this paper, surface waves in the presence of an infinite periodic array of obstacles of rectangular cross-section are considered. Rayleigh–Bloch surface waves are described by a localised wave motion which does not propagate energy away from the array. The periodicity of the array implies the existence of a cut-off frequency below which Rayleigh–Bloch surface waves may be sought. Such solutions are well established and Rayleigh–Bloch surface waves have been shown to exist for all rectangular cross-section. In the present paper, we generate examples of Rayleigh–Bloch surface waves for the more complicated case of frequencies lying above the first cut-off, such waves correspond mathematically to eigenvalues embedded in the continuous spectrum of the field operator. Numerical results are given for rectangular cross-sections based on an integral equation formulation of the problem. Finally, strong numerical evidence is given for embedded Rayleigh–Bloch waves that exist for a single family of rectangular cross-section above the second cut-off.

Keywords: Rayleigh–Bloch; Helmholtz equation; Periodic arrays; Continuous spectrum; Cut-off

1. Introduction

This paper is concerned with the solution of the two-dimensional Helmholtz equation for a function $\phi(x, y)$ in the presence of an infinite periodic array on which a Neumann condition ($\phi_n = 0$) is satisfied. Thus, it may be regarded as a problem in linear acoustics involving a diffraction grating, or a scalar problem in electromagnetics, or as a problem in linear surface gravity waves. This latter interpretation arises if we regard the lower half-space to be occupied by an ideal fluid under gravity bounded by a free surface, a horizontal bottom boundary at a depth h and an infinite periodic 'cliff' extending throughout the depth of the fluid. Then the linearised water wave equations

* Corresponding author. Tel.: +44 117 9287996; fax: +44 117 9287999.
E-mail address: richard.porter@bris.ac.uk (R. Porter).

0165-2125/$ – see front matter © 2005 Elsevier B.V. All rights reserved.
doi:10.1016/j.wavemoti.2005.05.005

allow us to extract the depth dependence from the three-dimensional harmonic potential function describing the flow, thereby reducing the problem to seeking solutions $\phi(x, y)$ satisfying

$$\phi_{xx} + \phi_{yy} + k^2\phi = 0$$

where k is the real positive root of

$$\omega^2 = gk \tanh kh$$

and a simple harmonic time variation of $e^{-i\omega t}$ has been assumed. Because of the authors' experience in the field, it will be in the surface gravity wave context that the paper will be developed although some readers may be more comfortable with the acoustic setting in which $k = \omega/c$, where c is the speed of sound.

In recent years, there has been a substantial body of work dedicated to an investigation of the conditions under which surface gravity waves are trapped by infinite periodic arrays of obstacles. This has been prompted by the discovery of Callan et al. [1] of the existence of trapped modes about a circular cylinder placed on the centreline of an open-ended water-filled channel. Such trapped modes describe motions of finite energy localised in space in the vicinity of the cylinder. By reflections in the channel walls they also correspond to localised standing waves about an infinite periodic array of identical circular cylinders. The existence of trapped modes about any symmetrical obstacle (such as a circular cylinder) placed on the centreline of the channel can be made plausible by the following argument. By considering antisymmetric wave motions about the channel centreline and using separation of variables far away from the obstacle it can be demonstrated that no outward propagating waves can exist provided the wavenumber k (where $k = 2\pi/\lambda$ and λ is the wavelength) is below a *cut-off* value of $\pi/2d$, where $2d$ is the width of the channel. It is, therefore, reasonable to seek trapped modes in the presence of a cylinder in the parameter region $k < \pi/2d$ and in fact a rigorous proof of the existence of antisymmetric channel trapped modes about symmetric obstacles has been given by Evans et al. [9].

The existence of trapped modes is less clear when either the wavenumber, k, is chosen to lie above the cut-off for the channel, or when the obstacle itself is not symmetric with respect to the channel centreline. In both these cases waves are able to propagate along the channel to infinity and there is no guarantee that localised wave fields will exist. Nevertheless, Evans et al. [9] were able to show that trapped modes could occur for a thin vertical plate aligned with the channel walls but moved from the centre of the channel. It was subsequently shown by Davies and Parnovski [3] (also see Groves [10]) that the existence of these trapped modes can be proved rigorously, since there are also cut-off wavenumbers that exist for particular problems involving thin plates aligned with channel walls below which trapped modes may be found. Very recently, Linton et al. [12] have found trapped modes using a numerical technique for more general obstacles which are not symmetrically placed in the channel.

The first example of trapped modes occurring *above* a cut-off was shown numerically by Evans and Porter [8] who considered the case of a circular cylinder on the channel centreline but with wavenumber k above the first channel cut-off but below the second channel cut-off such that $\pi/2d < k < 3\pi/2d$. Trapped modes above the cut-off are termed *embedded* trapped modes, since they are mathematically equivalent to the existence of an eigenvalue of the two-dimensional Laplacian operator $-\nabla^2$ which lies in the continuous spectrum of the operator, in the case discussed above for antisymmetric motions about a symmetric obstacle this is $k \in [\pi/2d, \infty)$. Whereas trapped modes below the cut-off (or below the continuous spectrum) occur for a large class of symmetrical obstacles, the embedded trapped mode of Evans and Porter [8] was shown to occur at a single precise cylinder radius and at a single wavenumber. More recently, it has been shown by McIver et al. [15] that the circular cylinder lies on a branch of trapped mode values for a class of symmetrical obstacle in which two geometric parameters are allowed to vary simultaneously. For example, by considering elliptical cylinder cross-sections $(x/a)^2 + (y/b)^2 = 1$, embedded trapped modes were shown to exist for a family of ellipses given by $a = a(b)$, whence trapped mode wavenumbers are given by $k = k(b)$. This characteristic of embedded trapped modes, namely that by changing one of the parameters in the problem and being able to adjust another in the appropriate fashion in order to retain a trapped mode, is an argument central to the present work.

The new feature presented in this paper is the extension of the concept of embedded trapped modes, now well established for channel problems, to Rayleigh–Bloch surface waves. A discussion of Rayleigh–Bloch waves in the diffraction-grating context is given by Wilcox [20]. Because of the correspondence between the acoustic problem and the depth-extracted surface gravity wave problem, the discussion in Wilcox also applies in the gravity wave context provided a Neumann condition is assumed on the periodic structure. Rayleigh–Bloch surface waves describe a localised or trapped wave in the presence of infinite periodic arrays of cylinders and are characterised by a dominant wavenumber of motion, β, along the array. The channel trapped modes referred to previously may be regarded as a special case of a Rayleigh–Bloch surface wave for which $\beta = \pi/2d$, where $2d$ refers to the spacing between adjacent cylinders in the array, when a standing wave solution is encountered. These are commonly referred to as Neumann trapped modes on account of the Neumann conditions satisfied by the field potential on the channel walls. A different type of standing wave solution occurs for $\beta = 0$ and are referred to in the literature as Dirichlet trapped modes; channel modes for which the condition on the channel walls are of the Dirichlet type. These modes have also been investigated by, for example, Evans and Porter [8]. See also Maniar and Newman [13] and Evans and Linton [7].

Using separation of variable arguments similar to those already described for channel trapped modes, it is possible to argue that a cut-off exists for the problem of Rayleigh–Bloch surface waves. Thus, there is a range of wavenumber k, given by $0 < k < \beta \leq \pi/2d$, for which waves cannot propagate away from the array. This argument has led to the discovery of surface waves along a variety of cylinder cross-sections including circular cylinders, rectangular blocks, thin plates and more general cross-sections (see Porter and Evans [17] for a general review). Rayleigh–Bloch surface waves were also shown by Porter and Evans [17] to be important in determining trapped modes for channels spanned by an arbitrary number of periodically spaced cylinders whilst the corresponding wavenumbers at which they occur have been shown by Utsunomiya and Eatock-Taylor [19] to be closely related to the phenomenon of near-trapping occurring in the scattering of waves by finite arrays of cylinders.

The purpose of the present work, therefore, is to investigate the existence of Rayleigh–Bloch surface waves *above* the cut-off and in accordance with the terminology used, such solutions will be called embedded Rayleigh–Bloch modes. The motivation for the existence of such modes is now clear. Results from McIver et al. [15] have established the existence of embedded channel trapped modes corresponding to $\beta = 0$ and $\pi/2d$ for plates and rectangular blocks having particular dimensions and occurring at specific values of k above the cut-off. By varying β from these values in the range $0 < \beta < \pi/2d$ and simultaneously also varying a geometrical parameter of the problem (such as plate length, for example), we may reasonably expect that the embedded mode is preserved. This is precisely the procedure we employ and apply it here to arrays of rectangular blocks, for which the simplicity of the geometrical configuration lends itself to powerful analytical techniques similar to those used previously in Evans and Fernyhough [5].

The existence of embedded Rayleigh–Bloch surface waves with $k = k(\beta)$ $(k > \beta)$ for a given periodic geometry has profound implications for the corresponding scattering of an incident wave by that geometry. Thus, for those particular values of k, β, to the scattered field due to a wave making an angle $\cos^{-1}(k/\beta)$ with the axis of the periodic array may be added any multiple of the Rayleigh–Bloch surface wave solution, thus rendering the scattering problem non-unique.

As mentioned at the beginning of this section, this problem also has an interpretation in electromagnetic theory and there is a large body of literature dedicated to the study of surfaces waves (guided waves or slow waves as they are sometimes called) in the application to microwave devices. In particular, microwaves devices including periodic elements are used to generate surface waves, which have the property that their phase speed, defined as $v_{\mathrm{p}} = \omega/\beta$, is slower than the speed of light, $c_{\mathrm{l}} = \omega/k$, for waves below the cut-off, $k < \beta$. This feature enables interaction between these travelling surface waves or 'slow waves' and electron beams which typically can only travel at 10 or 20% of the speed of light (see Chaterjee [2], chapter 9 or Elliot [4], p. 423, for example). The present work which focusses on $k > \beta$, therefore demonstrates that surface waves may also exist having phase speeds *greater* than the speed of light. It is not clear what implications this may have for the design of microwave devices and whether this new property can be harnessed for useful applications.

In Section 2, the governing equations that describe Rayleigh–Bloch surface waves are established in terms of a two-dimensional complex scalar field potential. Since the potential satisfies homogeneous conditions it may be modified by an arbitrary complex constant and a careful choice of the phase of this constant is made that is crucial in identifying how Rayleigh–Bloch solutions are to be determined from the subsequent formulation. In Section 3, eigenfunction expansions for the potential in two rectangular subdomains are derived with particular attention drawn to the number of wave-like modes present in each region. These are crucial in determining where possible embedded Rayleigh–Bloch solutions may lie in (k, β) parameter space and a heuristic wide-spacing argument described in Section 4 shows why this is so. In Section 5, the solution is formulated in terms of integral equations for unknown functions relating to velocities across gaps in a manner similar to Evans and Fernyhough [5]. These show that Rayleigh–Bloch waves above the first cut-off correspond to the vanishing of a real 2×2 determinant plus the satisfaction of a real side condition. It is the realness of both these conditions that allows solutions to be found and occurs as a direct consequence of the scaling in the potential chosen at the outset. In Section 6, the method of solution for the integral equations is described being based on a Galerkin technique similar to that used in Evans and Fernyhough [5]. Numerical results are given in Section 7, where embedded Rayleigh–Bloch waves above the first cut off are shown to correspond to the crossing of two curves in a two-dimensional plane. In Section 8, a consideration of Rayleigh–Bloch waves above the second cut-off, where existence is anticipated on account of the number of geometrical parameters available. It is found numerically that there is indeed one such family of solutions for which this new type of mode exists. Finally, some conclusions are drawn in Section 9 in which the practical importance of these new types of embedded surface waves is discussed with reference to scattering problems and guided or slow waves in microwave theory.

2. Governing equations

Identical rectangular blocks each uniform in cross-section, length $2a$ and width $2b$, are arranged to form an infinite linear periodic array of periodicity $2d$ and placed in an ideal fluid of constant depth h (see Fig. 1). Adjacent blocks are separated by a distance $2c$ such that $b + c = d$. Cartesian coordinate are chosen with $z = 0$ coinciding with the mean free surface of the fluid and z measured vertically downwards. Time harmonic motion of frequency $\omega/2\pi$ is assumed, and since the blocks extend uniformly throughout the depth we may write the linearised velocity potential Φ as

$$\Phi(x, y, z, t) = \mathrm{Re}\{\phi(x, y) \cosh k(z - h) \mathrm{e}^{-\mathrm{i}\omega t}\}$$

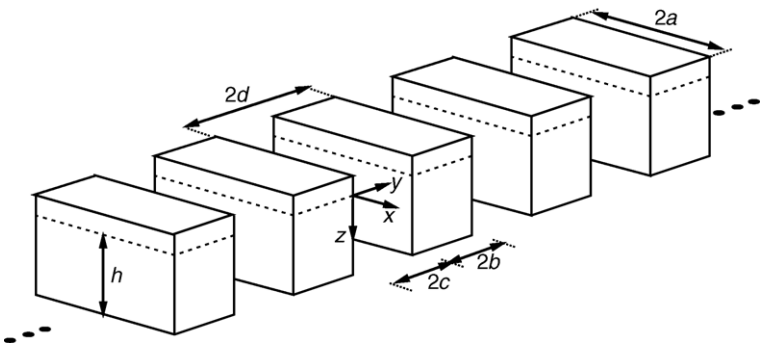

Fig. 1. Coordinate system and dimensions for a periodic array of rectangular blocks.

where k is the real positive root of the linear dispersion relation

$$\frac{\omega^2}{g} = k \tanh kh$$

and g is gravitational acceleration. In the context of acoustics, this equation is replaced by $k = \omega/c_v$, where c_v is the speed of sound in the fluid. The two-dimensional complex velocity potential $\phi(x, y)$ satisfies

$$(\nabla^2 + k^2)\phi(x, y) = 0, \tag{2.1}$$

in the fluid where ∇^2 is the two-dimensional Laplacian,

$$\frac{\partial \phi}{\partial n} = 0, \quad \text{on solid boundaries} \tag{2.2}$$

and

$$\phi \to 0, \quad \text{as } |x| \to \infty. \tag{2.3}$$

It is well known, see, for example, Evans and Fernyhough [5], that the periodicity of the infinite array implies a Floquet relation for the solution given by

$$\phi(x, y + 2md) = \mathrm{e}^{2\,\mathrm{i}m\beta d}\phi(x, y), \quad m \in \mathbb{Z} \tag{2.4}$$

for some real parameter β. This condition allows one to confine attention to any rectangular strip of width $2d$ containing a single period of the infinite array by imposing coupled conditions on two parallel boundaries of the strip. For example,

$$\phi(x, 2d) = \mathrm{e}^{2\mathrm{i}\beta d}\phi(x, 0), \qquad \phi_y(x, 2d) = \mathrm{e}^{2\mathrm{i}\beta d}\phi_y(x, 0). \tag{2.5}$$

Once $\phi(x, y)$ has been determined in the strip $S_0 = \{-\infty < x < \infty,\ 0 \le y \le 2d\}$, it can be extended to the rest of the fluid domain using (2.4).

The task is to find values of $k(\beta)$ for prescribed values of β for which (2.1)–(2.3) are satisfied by some non-trivial function $\phi(x, y)$. Such solutions are known as Rayleigh–Bloch surface waves in the context of electromagnetics, although Evans and Fernyhough [5] chose to call them edge waves in accordance with the terminology used for related wave phenomena in water waves.

We need only consider values of β in the interval $0 \le \beta < \pi/2d$, since it can easily be confirmed that if $k(\beta)$ is a solution then so is $k(\pi/d - \beta)$, $k(\beta + j\pi/d)$ for $j \in \mathbb{Z}$. (see, for example, §3 in Porter and Porter [18]). Rayleigh–Bloch waves have been shown to exist for a wide class of obstacle cross-section when $0 < k < \beta \le \pi/2d$ and the purpose of this paper is to construct Rayleigh–Bloch waves in the case $k > \beta$. The difference between these two cases is discussed later in this section.

The symmetry of the infinite array about lines $y = c + 2jd$, $j \in \mathbb{Z}$ plays an important role in determining solutions for $k > \beta$. Solutions of the homogeneous Eqs. (2.1)–(2.3) may be determined to within an arbitrary multiplicative complex constant and we can use the symmetry of the infinite array to scale the solution by a phase factor which turns out to be beneficial in later calculations. First, we introduce a new origin at $y' = y - c = 0$ which is located half way between adjacent blocks in the array. Then if $\phi(x, y')$ is a solution of (2.1)–(2.4) so is $\overline{\phi(x, -y')}$ and, assuming that these functions are linearly dependent, they may be related by an arbitrary constant, C, say, whence

$$\phi(x, y') = C\overline{\phi(x, -y')}.$$

Replacing y' by $-y'$ shows that $|C| = 1$ in the above. Since the function $\phi(x, y)$ is the solution of a homogeneous system of equations and boundary conditions, it may be scaled by an arbitrary constant and therefore we choose to

rescale with $C = 1$ so that

$$\phi(x, y') = \overline{\phi(x, -y')} \tag{2.6}$$

is satisfied. The complex potential ϕ is now decomposed into its real and imaginary parts by writing

$$\phi(x, y') = \phi^{\mathrm{s}}(x, y') + \mathrm{i}\phi^{\mathrm{a}}(x, y') \tag{2.7}$$

from which (2.6) may be used to show that

$$\phi^{\mathrm{s}}(x, y') = \phi^{\mathrm{s}}(x, -y'), \qquad \phi^{\mathrm{a}}(x, y') = -\phi^{\mathrm{a}}(x, -y'). \tag{2.8}$$

A similar decomposition was used in Porter and Evans [17]. The choice of scaling of the potential ϕ has allowed us to identify the real and imaginary parts of ϕ with its symmetric and antisymmetric components, respectively, which explains the use of superscripts s and a in the notation in (2.8). It follows that the components ϕ^{s} and ϕ^{a} satisfy, respectively, Neumann and Dirichlet conditions on the line $y' = 0$ (or $y = c$). Note that using the form of ϕ given by (2.7) in (2.4) with $m = 1$ and taking real and imaginary parts results in

$$\left.\begin{aligned} \phi^{\mathrm{s}}(x, c + 2d) &= \cos(2\beta d)\phi^{\mathrm{s}}(x, c) - \sin(2\beta d)\phi^{\mathrm{a}}(x, c) \\ \phi^{\mathrm{a}}(x, c + 2d) &= \sin(2\beta d)\phi^{\mathrm{s}}(x, c) + \cos(2\beta d)\phi^{\mathrm{a}}(x, c) \end{aligned}\right\}$$

with a similar pair of equations for $\phi_y^{\mathrm{s,a}}$. These coupled boundary conditions which now apply to a problem posed on the strip $S_c = \{-\infty < x < \infty,\ c < y < c + 2d\}$ decouple in two cases. First, when $\beta = 0$ to give

$$\phi^{\mathrm{s,a}}(x, c + 2d) = \phi^{\mathrm{s,a}}(x, c), \qquad \phi_y^{\mathrm{s,a}}(x, c + 2d) = \phi_y^{\mathrm{s,a}}(x, c)$$

and secondly with $\beta = \pi/2d$ to give

$$\phi^{\mathrm{s,a}}(x, c + 2d) = -\phi^{\mathrm{s,a}}(x, c), \qquad \phi_y^{\mathrm{s,a}}(x, c + 2d) = -\phi_y^{\mathrm{s,a}}(x, c).$$

Combining these identities in turn with (2.8) shows that the functions ϕ^{s} and ϕ^{a} satisfy Neumann and Dirichlet conditions (respectively) on *both* lines $y = c$ and $y = c + 2d$. Note that when $\beta = 0$ and $k < \pi/d$, it is known that $\phi^{\mathrm{s}} \equiv 0$, whilst when $k < \beta = \pi/2d$, $\phi^{\mathrm{a}} \equiv 0$ (see McIver and Linton [14].) Moreover, the decoupling of the problem in the cases $\beta = 0$ and $\beta = \pi/2d$ has some profound implications on the nature of the existence of Rayleigh–Bloch solutions which will be referred to later in this section.

The final step in the formulation of the problem comes from consideration of independent motions that are symmetric and antisymmetric about the line $x = -a$. We concentrate here on symmetric motions, such that

$$\phi_x = 0, \quad \text{on } x = -a. \tag{2.9}$$

The corresponding condition for antisymmetric motions is $\phi = 0$ on $x = -a$.

3. Eigenfunction expansions

The governing equations are now in place. To summarise, we seek non-trivial functions $\phi(x, y)$ in the semi-infinite strip $-a \le x < \infty$, $0 \le y \le 2d$ satisfying (2.1)–(2.3), (2.5), (2.6) and (2.9) for a given β in the interval $0 \le \beta \le \pi/2d$. The solution may be constructed using separation of variables in two rectangular sub-domains of the

strip S_0. First, in the inner region, $-a \le x \le 0$, bounded by the sides of adjacent blocks we represent the potential by writing

$$\phi(x, y) = \sum_{n=0}^{\infty} A_n \cosh \alpha_n (x + a) \psi_n(y) \tag{3.1}$$

where A_n are coefficients to be determined,

$$\psi_n(y) = \epsilon_n^{1/2} \mathrm{i}^n \cos p_n y, \quad p_n = \frac{n\pi}{2c}, \quad \epsilon_n = \begin{cases} 1, & n = 0, \\ 2, & n \ge 1 \end{cases} \tag{3.2}$$

and $2b = 2(d - c)$ is the thickness of the block. Also,

$$\begin{aligned} &\alpha_n = (p_n^2 - k^2)^{1/2} > 0, \quad n = P, P + 1, \ldots; \quad \alpha_n = -\mathrm{i}k_n, \quad \text{where} \\ &k_n = (k^2 - p_n^2)^{1/2} > 0, \quad n = 0, \ldots, P - 1. \end{aligned} \tag{3.3}$$

and $P = 1 + [2kc/\pi]$ where $[x]$ represents the integer part of x. Clearly, $k_0 \equiv k > 0$ and so $P \ge 1$. The first P terms in the summation in (3.1), therefore represent standing wave-like modes between the blocks and there is at least one such mode.

In the outer region, $x \ge 0$, extending to infinity we write

$$\phi(x, y) = \sum_{n=-\infty}^{\infty} B_n \mathrm{e}^{-\gamma_n x} \Psi_n(y) \tag{3.4}$$

where B_n are also coefficients to be determined and

$$\Psi_n(y) = \mathrm{e}^{\mathrm{i}\beta_n (y-c)}, \quad \text{with } \beta_n = \beta + n\pi/d \tag{3.5}$$

such that (2.5) is satisfied and

$$\begin{aligned} &\gamma_n = (\beta_n^2 - k^2)^{1/2} > 0, \quad n \notin \{Q_-, \ldots, Q_+\}; \quad \gamma_n \equiv -\mathrm{i}\kappa_n, \quad \text{where} \\ &\kappa_n = (k^2 - \beta_n^2)^{1/2} > 0, \quad n \in \{Q_-, \ldots, Q_+\}, \end{aligned} \tag{3.6}$$

where

$$Q_\pm = \left[\frac{d(\pm k - \beta)}{\pi} \right].$$

The total number of wave-like modes present in the expansions (3.4) is given by

$$Q = 1 + Q_- + Q_+.$$

When $0 < k \le \beta \le \pi/2d$, $Q = 0$ and all modes in $x > 0$ decay exponentially with increasing x in (3.4).

Note also the orthogonality relations

$$\frac{1}{2d} \int_0^{2d} \Psi_n(y) \overline{\Psi_m(y)} \, \mathrm{d}y = \frac{1}{2c} \int_0^{2c} \psi_n(y) \overline{\psi_m(y)} \, \mathrm{d}y = \delta_{mn}, \tag{3.7}$$

where δ_{mn} is the Kronecker delta. Crucially, the eigenfunctions $\psi_n(y)$ and $\Psi_n(y)$ defined for the inner and outer regions, respectively, have been scaled such that their real parts are even about $y = c$ and their imaginary parts are odd functions about $y = c$. From the form of the potential assumed in (2.7) this scaling immediately ensures that

the coefficients A_n in (3.1) are real for all n whilst B_n in (3.4) are also real for values of $n \notin \{Q_-, \ldots, Q_+\}$ (i.e. for all decaying modes).

We have already seen that no wave-like modes exist ($Q = 0$) in the outer region extending to infinity provided $0 < k \leq \beta \leq \pi/2d$ and in this region of (k, β) parameter space (2.3) is automatically satisfied. This observation allowed Evans and Linton [6] and later Evans and Fernyhough [5] and Porter and Evans [17] to construct Rayleigh–Bloch waves for several families of cylinder cross-section. We need to consider carefully how we can motivate the construction of a solution for which it is possible to satisfy (2.3) when $k > \beta$. For this we need to classify the number of wave-like terms in the expansions in the two regions throughout the (k, β) plane, recalling that we only need to consider the interval $0 \leq \beta \leq \pi/2d$.

Fig. 2 summarises the numbers, P and Q, of wave-like modes present in the inner region $-a \leq x < 0$ and in the outer region, $x \geq 0$, respectively, throughout the (k, β) plane. The short dashed horizontal lines represent cut-off wavenumbers in the inner region between the blocks. As k increases across one of these lines, the number of wave-like modes, P, increases by one. The longer dashed diagonal lines represent similar cut-off wavenumbers in the outer region $x > 0$. Starting with a value of $Q = 0$ in $0 < k \leq \beta \leq \pi/2d$, the value of Q increases by one as k increases across each such line. Thus, each part of (k, β) parameter space can be characterised by the number of wave-like modes present in each region by labelling it (P, Q) in Fig. 2.

The vertical lines $\beta = 0$ and $\pi/2d$ require special consideration, since in these two cases we have already shown that the problem decouples into either Neumann or Dirichlet problems for potentials labelled ϕ^{s} and ϕ^{a} that are symmetric and antisymmetric, respectively, about both the parallel lines $y = c$ and $y = c + 2d$ between which a

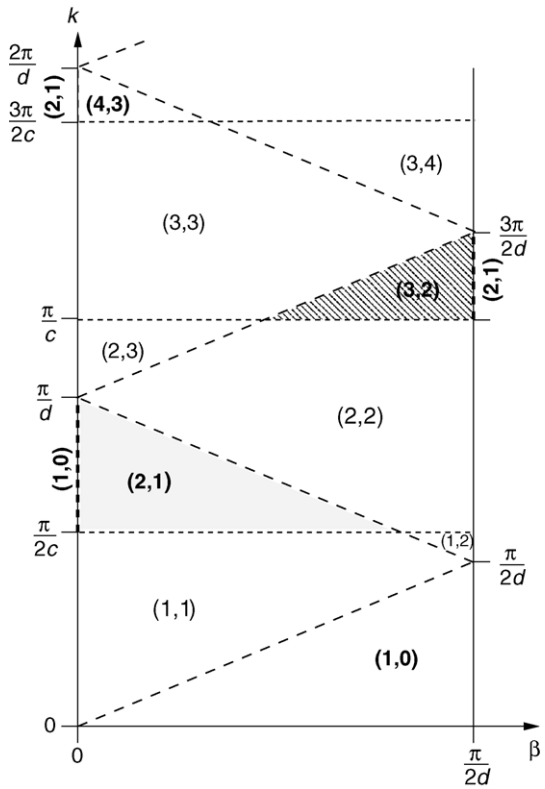

Fig. 2. The number of wave-like modes in the inner and outer regions, (P, Q), represented in (k, β) space for a periodic array of rectangular blocks.

block is centrally placed. Thus, the problem reduces, in these cases, to a single block of width $2b$ in a channel of width $2d$. Embedded Rayleigh–Bloch modes have previously been considered in these two cases first by Evans and Porter [8] then by McIver et al. [15] and Linton et al. [12] where they are called Neumann ($\beta = \pi/2d$) and Dirichlet ($\beta = 0$) embedded trapped modes. However, it is a useful exercise to demonstrate how the Rayleigh–Bloch formulation of the problem for general β reduces to these special cases. Because of the symmetry properties built into the eigenfunctions $\psi_n(y)$ and $\Psi_n(y)$, the general expansions for the potential in the two regions also separate for these values of $\beta = 0$ and $\pi/2d$. Thus, the $\psi_{2n}(y)$ are symmetric across $y = c$ and the $\psi_{2n+1}(y)$ are antisymmetric across $y = c$. So in $-a \le x \le 0$

$$\phi^{\mathrm{s}}(x, y) = \sum_{n=0}^{\infty} A_{2n} \cosh \alpha_{2n}(x + a)\psi_{2n}(y) \tag{3.8}$$

whilst

$$\phi^{\mathrm{a}}(x, y) = \sum_{n=0}^{\infty} A_{2n+1} \cosh \alpha_{2n+1}(x + a)\psi_{2n+1}(y) \tag{3.9}$$

and in each case the value of P representing the number of wave-like modes, needs to redefined accordingly to $P^{\mathrm{s}} = 1 + [kc/\pi]$, $P^{\mathrm{a}} = [\frac{1}{2} + kc/\pi]$.

In the outer region $x > 0$, when $\beta = \pi/2d$, we find that $\beta_{-n-1} = -\beta_n$, so that $\gamma_{-n-1} = \gamma_n$ and this allows us to write

$$\phi^{\mathrm{s}}(x, y) = \sum_{n=0}^{\infty} B_n^{\mathrm{s}} \mathrm{e}^{-\gamma_n x} \cos \beta_n(y - c) \tag{3.10}$$

where $B_n^{\mathrm{s}} = B_n + B_{-n-1}$ are revised unknown coefficients. Since the sum now starts at zero the number of wave-like modes is now given by $Q^{\mathrm{s}} = 1 + Q_+$ in this case.

When $\beta = 0$, we have $\beta_{-n} = \beta_n$, and thus $\gamma_n = \gamma_{-n}$ also and so

$$\phi^{\mathrm{a}}(x, y) = \sum_{n=1}^{\infty} B_n^{\mathrm{a}} \mathrm{e}^{-\gamma_n x} \sin \beta_n(y - c) \tag{3.11}$$

where $B_n^{\mathrm{a}} = B_n + B_{-n}$ are new unknown coefficients. In the expansion above the sum starts at $n = 1$ and so here the number of wave-like modes in $x > 0$ is given by $Q^a = Q_+$. In general, on the lines $\beta = 0$ and $\beta = \pi/2d$, the values of P and Q are reduced. Particular intervals of k for these two values of β for which $P > Q$ are indicated on Fig. 2 by bold labels rotated through 90°. Notice that we have not considered ϕ^{a} for $\beta = \pi/2d$ nor ϕ^{s} for $\beta = 0$. The reason for this is that, in both these cases, the number of wave-like modes in $x > 0$ is one more than in the two cases that have been detailed above and there are, therefore, no corresponding intervals of k for which $P > Q$. To summarise then, for $\beta = \pi/2d$ we confine attention to the Neumann problem for ϕ^{s} and on $\beta = 0$, the Dirichlet problem for ϕ^{a}.

We are particularly interested in regions of (k, β) parameter space in which $P > Q$ for reasons that will be explained in the following section.

4. Wide-spacing arguments

We confine attention to regions of (k, β) space where $P > Q \ge 1$ which are labelled bold in Fig. 2. In fact, $P = Q + 1$ in every such region and sketched in Fig. 2 are regions labelled (4, 3), (3, 2), (2, 1), but the existence of each of these regions is dependent on the width of the rectangular block unlike the (1, 0) region. Thus, the triangular (2, 1) region only exists provided $c > \frac{1}{2}d$, the (3, 2) region exists provided $c > \frac{2}{3}d$ and so on.

We shall adopt the arguments used by McIver et al. [15] to motivate the existence of their embedded mode to justify the possible existence of a Rayleigh–Bloch mode, whenever there are more wave-like modes in the inner region, $-a \le x \le 0$, than in the outer region, $x > 0$.

Consider a region of (k, β) parameter space which is labelled $(Q+1, Q)$, for $Q \ge 1$, i.e. there is at least one possible wave-like mode in the outer region. As a first step consider the case where the blocks extend from $-\infty < x < 0$ and construct a sequence of $P = Q+1$ scattering problems involving waves propagating in the positive x direction from $x = -\infty$ of the form $\mathrm{e}^{\mathrm{i}k_m x}\psi_m(y)$, $m = 0, \ldots, Q$. Let $\phi_m(x, y)$ be the potential associated with each scattering problem. Then $\phi_m(x, y)$ satisfies (2.1), (2.2) and (2.4), but instead of (2.3) and (2.9) we have

$$\phi_m(x, y) \sim \begin{cases} \mathrm{e}^{\mathrm{i}k_m x}\psi_m(y) + \displaystyle\sum_{n=0}^{Q} R_{m,n}\mathrm{e}^{-\mathrm{i}k_n x}\psi_n(y), & x \to -\infty \\ \displaystyle\sum_{n=0}^{Q-1} T_{m,n}\mathrm{e}^{\mathrm{i}\kappa_n x}\Psi_n(y), & x \to \infty \end{cases}$$

where $R_{m,n}$ and $T_{m,n}$ are the nth modal reflected and transmitted wave coefficients due to the mth incident wave mode. Next, define a new potential $\chi(x, y)$, being the combination

$$\chi(x, y) = \sum_{n=0}^{Q} d_n \phi_n(x, y)$$

where the coefficients, d_n, are to be chosen to satisfy

$$\sum_{n=0}^{Q} d_n T_{m,n} = 0, \quad m = 0, \ldots, Q-1$$

which can be done to within an arbitrary multiplicative constant. Then

$$\chi(x, y) \sim \begin{cases} \displaystyle\sum_{n=0}^{Q}\left(d_n\mathrm{e}^{\mathrm{i}k_n x} + \sum_{m=0}^{Q} d_m R_{m,n}\mathrm{e}^{-\mathrm{i}k_n x}\right)\psi_n(y), & x \to -\infty \\ 0, & x \to \infty \end{cases}$$

which has the desired decay at $x \to \infty$. In order to apply this to a periodic array of blocks of length $2a$, $a \gg 1$, we use a wide-spacing argument in a similar fashion to McIver et al. [15]. A Rayleigh–Bloch mode for blocks of length $2a$ is approximated by imposing the condition $\chi_x|_{x=-a} = 0$ which in turn requires

$$\sum_{n=0}^{Q}\left(d_n\mathrm{e}^{-2\,\mathrm{i}k_n a} - \sum_{m=0}^{Q} d_m R_{m,n}\right) = 0$$

to be satisfied. This is certainly the case if

$$d_n\mathrm{e}^{-2\,\mathrm{i}k_n a} = \sum_{m=0}^{Q} d_m R_{m,n}, \quad m = 0, \ldots, Q$$

holds. However, this argument requires that $Q+1$ equations are met simultaneously, and we would therefore expect that at least $Q+1$ independent parameters are required to satisfy this.

For example, with $Q = 1, d_0 = -d_1 T_{1,0}/T_{0,0}$ and then the approximate conditions to be satisfied for the existence of a Rayleigh–Bloch mode turn out to be

$$\left.\begin{aligned} \mathrm{e}^{-2\mathrm{i}k_0 a} &= R_{0,0} - \frac{T_{0,0}R_{0,1}}{T_{1,0}}, \\ \mathrm{e}^{-2\mathrm{i}k_1 a} &= R_{1,1} - \frac{T_{1,0}R_{1,0}}{T_{0,0}}. \end{aligned}\right\} \tag{4.1}$$

This formula may be applied in any (2, 1) region of (k, β) space (see Fig. 2). In the case previously discussed, McIver et al. [15] considered Rayleigh–Bloch waves in such a region, the line $\beta = \pi/2d$, with $\pi/d < k < 3\pi/2d$, for a thin plate where they are equivalent to Neumann trapped modes. The only independent parameters that can be varied in this case are k and a, but this is sufficient to simultaneously satisfy the two conditions above for particular values of k and a.

So far, examples of embedded waves have only been found in the special cases of $\beta = 0$ and $\pi/2d$. In the next section, we look for embedded modes for *arbitrary* β by confining attention to the region of parameter space shaded grey in Fig. 2 and given by $\pi/2c < k < \pi/d - \beta$ for $0 \le \beta \le \pi/c - \pi/2d$ which is above the first cut-off but below the second.

5. Integral equation formulation

Rather than using the wide-spacing arguments presented in the previous section which require the solution of a sequence of semi-infinite scattering problems and which only provide an approximate condition for the existence of Rayleigh–Bloch waves we seek Rayleigh–Bloch wave solutions directly using an integral equation formulation similar to Evans and Fernyhough [5].

An integral equation formulation is developed for the (2, 1) region of parameter space shaded grey in Fig. 2 and given by $\pi/2c < k < \pi/d - \beta$, $0 \le \beta \le \pi/c - \pi/2d$ which correspond to Rayleigh–Bloch waves above the first cut-off. The changes required to the formulation when we go above the second cut-off are given briefly in Section 8.

We start with the expansions for the potential in $-a \le x \le 0$ and $x \ge 0$ given by (3.1) and (3.4), respectively. In order to proceed, we match ϕ and ϕ_x from the two expressions for the potential along the common boundary $x = 0$ and $0 \le y \le 2c$ and must also impose no normal flow on $x = 0$ for $2c \le y \le 2d$. Following Evans and Fernyhough [5], we define

$$U(y) \equiv \phi_x|_{x=0} = \sum_{n=-\infty}^{\infty} B_n(-\gamma_n)\Psi_n(y) = \begin{cases} \sum_{n=0}^{\infty} A_n\alpha_n \sinh\alpha_n a\psi_n(y), & 0 \le y \le 2c, \\ 0, & 2c \le y \le 2d. \end{cases} \tag{5.1}$$

Multiplying by $\overline{\Psi_m(y)}$ and integrating over $0 \le y \le 2d$ gives

$$B_m = -(2\gamma_m d)^{-1} \int_0^{2c} U(y)\overline{\Psi_m(y)}\,\mathrm{d}y, \quad m = 0, \pm1, \pm2, \ldots, \tag{5.2}$$

where the fact that $U(y) = 0$ for $2c \le y \le 2d$ has been used. Again, multiplying (5.1) by $\overline{\psi_m(y)}$ and integrating now over $0 \le y \le 2c$ gives

$$A_m = (2\alpha_m c \sinh\alpha_m a)^{-1} \int_0^{2c} U(y)\overline{\psi_m(y)}\,\mathrm{d}y, \quad m = 0, 1, 2, \ldots. \tag{5.3}$$

Continuity of ϕ across $x = 0$ is expressed as

$$\sum_{n=-\infty}^{\infty}{}' B_n\Psi_n(y) = \sum_{n=0}^{\infty} A_n \cosh\alpha_n a\psi_n(y), \quad 0 \le y \le 2c \tag{5.4}$$

where we have chosen to set $B_0 = 0$, a requirement of the solution, and the prime denotes the term $n = 0$ is omitted from the summation. We later introduce an additional condition that tests if the condition $B_0 = 0$ has in fact been met. Substituting into (5.4) from (5.2) and (5.3) whilst extracting the $n = 0, 1$ terms from the right-hand side of (5.4) gives

$$(\mathcal{K}U)(y) \equiv \int_0^{2c} U(t)K(y,t)\,\mathrm{d}t = -A_0\cos k_0 a\psi_0(y) - A_1\cos k_1 a\psi_1(y), \quad 0 < y < 2c \tag{5.5}$$

where

$$K(y,t) = \sum_{n=-\infty}^{\infty}{}' \frac{1}{2\gamma_n d}\Psi_n(y)\overline{\Psi_n(t)} + \sum_{n=2}^{\infty}\frac{\coth\alpha_n a}{2\alpha_n c}\psi_n(y)\overline{\psi_n(t)}. \tag{5.6}$$

We let $u_n(t)$, $n = 0, 1$ satisfy

$$(\mathcal{K}u_n)(y) = \psi_n(y), \quad 0 < y < 2c \tag{5.7}$$

whence

$$U(t) = -A_0u_0(t)\cos k_0 a - A_1u_1(t)\cos k_1 a \tag{5.8}$$

satisfies (5.5). Note that $(\mathcal{K}u, v) = (u, \mathcal{K}v)$, where we have used the inner product notation

$$(u, v) = \int_0^{2c} u(y)\overline{v(y)}\,\mathrm{d}y,$$

and so the operator $\mathcal{K}$ is self-adjoint. Furthermore, it is readily shown that $(\mathcal{K}u, u) \geq 0$ and so $\mathcal{K}$ is a positive operator.

Using (5.8) in (5.3) with $m = 0, 1$ gives

$$\left.\begin{aligned} 2A_0k_0c\sin k_0a &= A_0S_{0,0}\cos k_0a + A_1S_{0,1}\cos k_1a \\ 2A_1k_1c\sin k_1a &= A_0S_{1,0}\cos k_0a + A_1S_{1,1}\cos k_1a \end{aligned}\right\} \tag{5.9}$$

where we have defined

$$S_{m,n} = (u_n, \psi_m), \quad n = 0, 1; m = 0, 1, \ldots \tag{5.10}$$

The $S_{m,n}$ can be shown to be real. This follows from the condition (2.6) we imposed on $\phi(x, y)$ from which we were able to make the decomposition in (2.7) with (2.8) into symmetric and antisymmetric parts about the line of symmetry, $y = c$. We can therefore make a corresponding decomposition of the function $U(y)$, writing

$$U(y') = U^{\mathrm{s}}(y') + \mathrm{i}U^{\mathrm{a}}(y'), \quad \text{where } U^{\mathrm{s}}(y') = U^{\mathrm{s}}(-y') \text{ and } U^{\mathrm{a}}(y') = -U^{\mathrm{a}}(-y')$$

and $y' = y - c$. By (5.8), a similar decomposition can be applied to the functions $u_i(y)$, $i = 0, 1$, since A_0 and A_1 have already been established as being real coefficients. Then

$$S_{m,n} = (u_n, \psi_m) = \epsilon_m^{1/2}\mathrm{i}^m\int_0^{2c}(u_n^{\mathrm{s}}(u) + \mathrm{i}u_n^{\mathrm{a}}(y))\cos\left(\frac{m\pi y}{2c}\right)\,\mathrm{d}y$$

and straightforward algebra shows that

$$(u_n, \psi_{2m}) = 2\epsilon_m^{1/2}\int_0^{c} u_n^{\mathrm{s}}(c-y)\cos\left(\frac{2m\pi y}{c}\right)\,\mathrm{d}y$$

whilst

$$(u_n, \psi_{2m-1}) = 2\sqrt{2}\int_0^c u_n^a(c-y)\sin\left(\frac{(2m-1)\pi y}{c}\right)\,\mathrm{d}y.$$

and hence $S_{m,n}$ are real for $n = 0, 1$ and for all $m = 0, 1, \ldots$.

Using (5.7) and the properties of $\mathcal{K}$ we have $S_{n,m} = (u_m, \mathcal{K}u_n) = (\mathcal{K}u_m, u_n) = \overline{(u_n, \mathcal{K}u_m)} = \overline{S_{m,n}} = S_{m,n}$. Furthermore, since $\mathcal{K}$ is a positive operator, $S_{n,n} \geq 0$, $n = 0, 1$ with equality only if $u_n = 0$.

For a Rayleigh–Bloch mode to exist we require that the pair of Eq. (5.9) written as

$$\begin{pmatrix} S_{0,0} - 2k_0 c\tan k_0 a & S_{0,1} \\ S_{1,0} & S_{1,1} - 2k_1 c\tan k_1 a \end{pmatrix}\begin{pmatrix} \hat{A}_0 \\ \hat{A}_1 \end{pmatrix} = \begin{pmatrix} 0 \\ 0 \end{pmatrix} \tag{5.11}$$

possess a non-trivial solution for $\hat{A}_0 = A_0\cos ka$, $\hat{A}_1 = A_1\cos k_1 a$. In other words, the determinant of the matrix must vanish, and so

$$\det(\mathbf{S}) = (S_{0,0} - 2k_0 c\tan k_0 a)(S_{1,1} - 2k_1 c\tan k_1 a) - S_{0,1}S_{1,0} = 0. \tag{5.12}$$

When this real equation is satisfied, values of $\hat{A}_0$, $\hat{A}_1$ can be found, being the eigenvector of the 2×2 matrix $\mathbf{S}$ in (5.11) corresponding to the zero eigenvalue.

In addition to the condition (5.12) being satisfied, we must reintroduce the corresponding values of A_0 and A_1 via (5.8) into (5.2) with $m = 0$ to ensure that there are no propagating wave modes in $x > 0$. Thus, we require the solution of (5.11) to satisfy

$$2\mathrm{i}\kappa_0 dB_0 = \{\hat{A}_0 P_{0,0} + \hat{A}_1 P_{0,1}\} = 0 \tag{5.13}$$

where we have written

$$P_{m,n} = (u_n, \Psi_m) = \int_0^{2c} u_n(y)\mathrm{e}^{-\mathrm{i}\beta_m(y-c)}\,\mathrm{d}y, \quad n = 0, 1. \tag{5.14}$$

In a similar fashion to before, we can use the decomposition of $u_i(y)$ into symmetric and antisymmetric parts to show that

$$P_{m,n} = 2\int_0^c [u_n^{\mathrm{s}}(c-y)\cos\beta_m y + u_n^{\mathrm{a}}(c-y)\sin\beta_m y]\,\mathrm{d}y$$

for $n = 0, 1$ and $m \in \mathbb{Z}$ and $P_{m,n}$ are therefore real. Thus, the condition (5.13) is real.

To summarise, in order to show the existence of a Rayleigh–Bloch wave, we must solve (5.7) for unknown functions $u_i(y)$, $i = 0, 1$, such that two real Eqs. (5.12) and (5.13) are simultaneously satisfied. Notice that the fact that we have to satisfy two conditions is consistent with the heuristic wide-spacing arguments presented at the end of the previous section.

6. Method of solution

Evans and Fernyhough [5] describe in detail how the approximation to the solution of the integral Eq. (5.7) can be made using a powerful Galerkin method. The procedure here is almost identical and only details are given to the derivation of the final system of equations.

We make approximations to $u_i(y)$ in the form

$$u_i(y) \approx \sum_{n=0}^{N} a_n^{(i)} v_n(y), \quad 0 \le y \le 2c$$

where the set of functions $\{v_n(y)\}$ are chosen to incorporate the expected $O(y^{-1/3}(2c-y)^{-1/3})$ behaviour in the functions $u_i(y)$, and to provide maximum simplification in the final system of equations. We choose

$$v_n(y) = \frac{\mathrm{i}^n n! \Gamma(1/6)}{2^{1/2}\pi\Gamma(n+1/3)(2yc)^{1/3}(2c-y)^{1/3}} C_n^{1/6}\left(\frac{y-c}{c}\right)$$

(see Evans and Fernyhough [5]) where $C_m^{\nu}(x)$ is an orthogonal Gegenbauer polynomial satisfying $C_m^{\nu}(x) = (-1)^m C_m^{\nu}(x)$. It can readily be seen that $v_{2m}(y)$ are real functions which are even about $y = c$, whilst $v_{2m+1}(y)$ are imaginary functions which are odd about $y = c$. This is precisely the property that is required of the functions $u_i(y)$.

Applying a Galerkin approximation to the integral Eq. (5.7) results in the algebraic system of equations

$$\sum_{n=0}^{N} a_n^{(i)} K_{m,n} = F_m^{(i)}, \quad m = 0, 1, \ldots, N$$

for the unknown coefficients, $a_n^{(i)}$, $i = 0, 1$. Here,

$$K_{m,n} = (\mathcal{K}v_n, v_m) = {\sum_{r=-\infty}^{\infty}}' \frac{1}{2\gamma_r d(\beta_r c)^{1/3}} J_{m+1/6}(\beta_r c) J_{n+1/6}(\beta_r c)$$
$$+ \sum_{r=2}^{\infty} E_{r,m,n} \frac{\coth \alpha_r a}{2\alpha_r c}\left(\frac{2}{\pi r}\right)^{1/3} J_{m+1/6}\left(\tfrac{1}{2}r\pi\right) J_{n+1/6}\left(\tfrac{1}{2}r\pi\right)$$

so that $K_{m,n} = K_{n,m}$ with $E_{r,m,n} = \frac{1}{2}[(-1)^r + (-1)^m][(-1)^r + (-1)^n]$ and

$$F_m^{(0)} = (\psi_0, v_m) = \frac{6}{2^{1/6}\Gamma(1/6)}\delta_{m0}, \qquad F_m^{(1)} = (\psi_1, v_m) = \begin{cases} 2^{1/2}\left(\dfrac{2}{\pi}\right)^{1/6} J_{m+1/6}\left(\dfrac{1}{2}\pi\right), & m \text{ odd} \\ 0, & m \text{ even} \end{cases}$$

The elements $S_{i,j}$ defined in (5.10) are approximated by

$$S_{i,j} \approx \sum_{n=0}^{N} a_n^{(j)} F_n^{(i)}, \quad i, j = 0, 1$$

and finally, from (5.13)

$$2\,\mathrm{i}\kappa_0 dB_0 \approx \sum_{n=0}^{N} \{\hat{A}_0 a_n^{(0)} + \hat{A}_1 a_n^{(1)}\} \frac{1}{(\beta c)^{1/6}} J_{n+1/6}(\beta c)$$

Notice that $K_{m,n}$ and $F_m^{(i)}$ are real and therefore so are $a_n^{(i)}$, $S_{i,j}$ and $2\,\mathrm{i}\kappa_0 dB_0$.

7. Results

Recall that our objective is to locate Rayleigh–Bloch waves above the first cut-off. That is, we seek values of $k(\beta)$ in the region $\pi/d - \beta < k < \pi/2c$, where $0 < \beta \leq \pi/d - \pi/2c$ which is the triangular (2, 1) region of (k, β) parameter space shaded grey in Fig. 2.

Locating embedded Rayleigh–Bloch waves for the case of a general rectangular array and for a general value of β is not straightforward due to the number of independent parameters that can be varied. For example, for some given value of β and non-dimensional block width, b/d, we can vary the remaining two parameters, kd and a/d, referring to the non-dimensional wavenumber and block length such that for particular pairs of kd and a/d the two real conditions (5.12) and (5.13) are met simultaneously. Consequently, it is extremely important to employ a systematic procedure to save on computational time and to ensure that all possible solutions have been found. We describe this procedure in detail below where the branch structure of the solutions is also revealed.

The first step is to compute results for $\beta = 0$ on the interval $\pi/2c < k < \pi/d$ which is non-empty provided $b/d < \frac{1}{2}$. The reason for starting with the line $\beta = 0, \pi/2c < k < \pi/d$ is that it is adjacent in (k, β) parameter space to the region in which we seek Rayleigh–Bloch waves above the first cut-off and that the solutions on this line correspond to *Dirichlet trapped waves* (refer to the discussion in Sections 2 and 4 in the case when $\beta = 0$). These are significantly easier to calculate for reasons that follow. First, Dirichlet trapped modes for $kd < \pi$ are below the first cut-off and are known to exist for all lengths a/d and for all widths of block in the interval $0 \leq b/d < \frac{1}{2}$ (see, for example, the introduction of Porter and Evans [8]). Secondly, Dirichlet trapped waves can be determined numerically by satisfying a single condition rather than two conditions simultaneously as is the case for Rayleigh–Bloch waves above the first cut-off. We explain briefly how this occurs. When $\beta = 0$, the full potential decouples into potentials, $\phi^{\mathrm{s,a}}$, that are symmetric and antisymmetric about the line $y = c$ as described in Section 2 whilst in Section 4 it is argued that it is the latter that is likely to give rise to trapped modes which satisfy a Dirichlet condition on $y = c$. A reworking of the integral equation formulation can be made for the function $\phi^{\mathrm{a}}(x, y)$ defined in (3.9) and (3.11), where for $\pi/2c < k < \pi/d$, there is one wave-like mode between adjacent blocks in the array and no wave-like modes away from the array. The same result can be obtained by setting all contributions to the solution that are symmetric about $y = c$ to zero in Section 5, resulting in $\hat{A}_0 = 0$, $P_{0,1} = S_{0,1} = 0$ and so $B_0 = 0$ is satisfied automatically whilst (5.10) reduces simply to

$$2k_1 c \tan k_1 a - S_{1,1} = 0 \tag{7.1}$$

in conjunction with the integral Eq. (5.7) using $n = 1$ only. Curves showing computed values of kd at which Dirichlet trapped waves occur with a/d for values of $b/d = 0, 0.15, 0.3, 0.45$ are shown in Fig. 3. This problem has also been considered by Shipway (private communication).

The next step in the procedure, now that Dirichlet trapped wave solutions corresponding to $\beta = 0$ have been established is to choose a non-zero value of $\beta = \epsilon > 0$ where ϵ is small. Since $\beta \neq 0$ there are now two conditions that need to be satisfied in order for a solution to exist. The first is given by (5.12) which states that the determinant of the 2×2 matrix $\mathbf{S}$ in (5.11) vanishes. This condition for $\beta > 0$ replaces (7.1) for $\beta = 0$. The additional condition is given by (5.13) which uses the resulting non-trivial values of $\hat{A}_0$ and $\hat{A}_1$. However, rather than having to look throughout the whole range of values of kd and a/d, for $\beta = \epsilon$, we know that the condition $\det(\mathbf{S}) = 0$ will be satisfied close to values computed for $\beta = 0$ shown in Fig. 3. Along each of these curves the value of B_0 can be monitored to see if it passes through a zero. Where it does pass through a zero both conditions (5.12) and (5.13) are satisfied simultaneously and we have numerically located an embedded Rayleigh–Bloch solution for $\beta = \epsilon$. These values are indicated on Fig. 3 by the boxes. The particular isolated values indicate the starting point of a branch of embedded Rayleigh–Bloch solution along the positive values of β. This branch can then be tracked numerically for a sequence of increasing values of β using the values found for $\beta = \epsilon$.

Results showing sets of values for which embedded Rayleigh–Bloch waves above the first cut-off occur are shown in Figs. 4 and 5. These results, like all other results in this paper, have been produced using a truncation

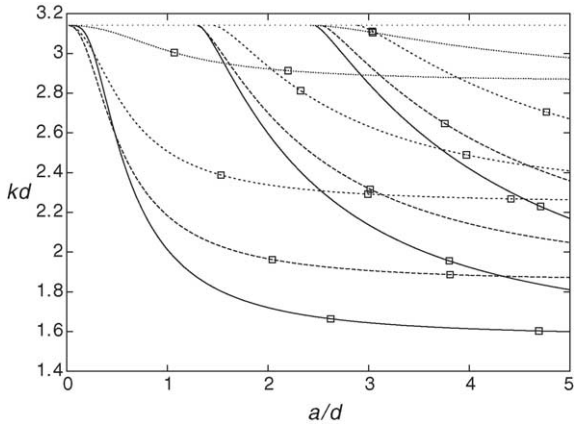

Fig. 3. Dirichlet trapped modes ($\beta = 0$) showing variation of kd with a/d for different block widths b/d: 0 (—), 0.15 (– –), 0.3 (- - -), 0.45 ($\cdots$). The boxes indicate the start of a branch into $\beta > 0$.

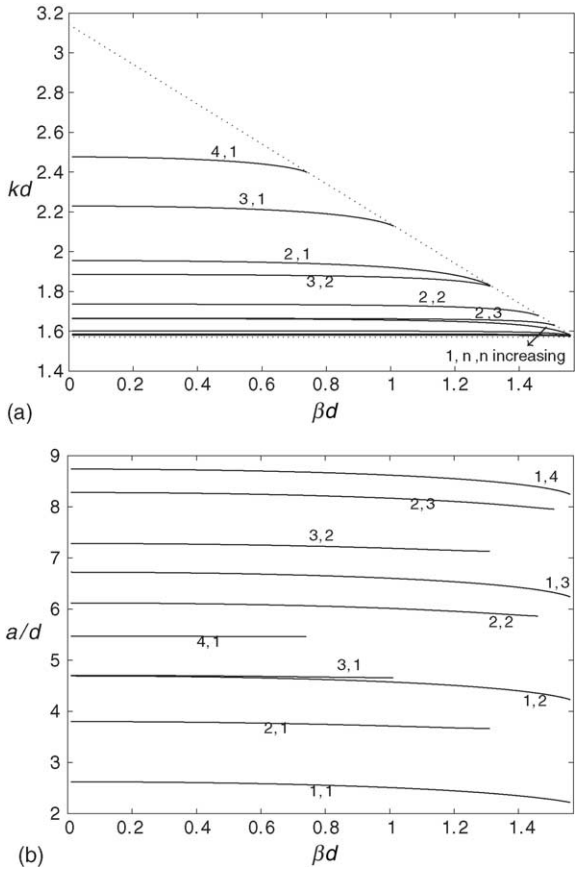

Fig. 4. Variation of (a) kd and (b) a/d with βd for arrays of thin plates ($b/d = 0$). Refer to the text for labelling.

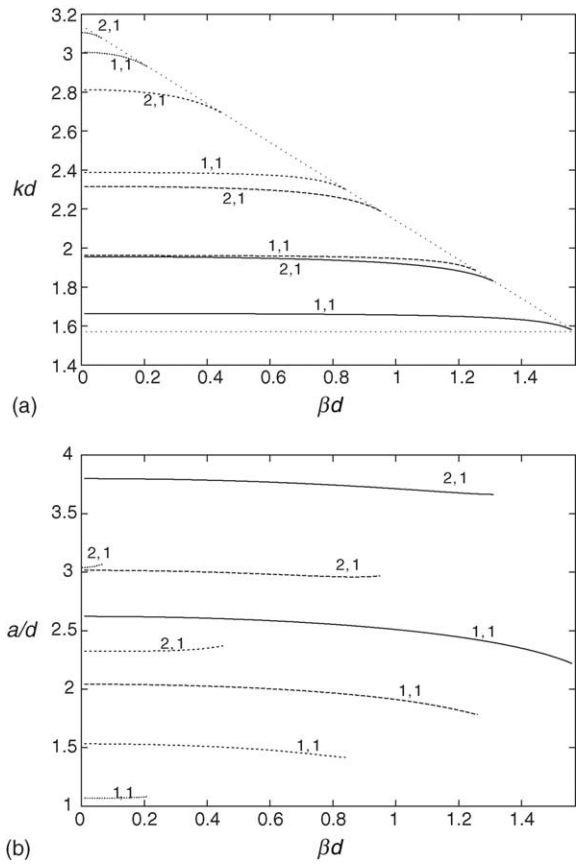

Fig. 5. Variation of (a) kd, (b) a/d with βd for Rayleigh–Bloch waves above the first cut-off for for different block widths b/d: 0 (—), 0.15 (– –), 0.3 (- - -), 0.45 (· · ·). Refer to text for labelling.

parameter $N = 10$ which gives at least five figure accuracy in all cases. This is the case even when the width of the rectangular block is reduced to zero ($b/d = 0$). Similar accuracy was reported in Evans and Fernyhough [5], although it should be noted that in the case of $b/d = 0$ the test functions used in the expansion for the unknown functions in Section 6 no longer correctly model the singular behaviour at the edge of the plate which is increased in strength to an inverse square-root singularity. Further confirmation of the results for $b/d = 0$ is provided by comparing with results using the residue calculus technique applicable for thin plates. These results form the basis for a future paper in which a rigorous proof of the existence of embedded Rayleigh–Bloch surface waves is established.

In Fig. 4(a and b) the variation of kd and a/d with the non-dimensionalised wavenumber βd is shown for arrays of thin plates ($b/d = 0$). There is an infinite sequence of branches of Rayleigh–Bloch wave solutions of which only the first few are shown in Fig. 4(a and b) and which can be classified with reference to the Dirichlet trapped mode results shown in Fig. 3. Each curve in Fig. 4(a and b) is a branch which originates from a boxed point in Fig. 3 and is labelled by a pair of integers. The first number in the pair indicates from which of the solid curves in Fig. 3, counting from left to right, the branch originates. The second number indicates the order along each curve from which the branch originates. Thus, the sequence of curves $1, n$, $n = 1, 2, 3, 4$ in Fig. 4(a and b) all branched from values of kd and a/d given by the boxed points on the leftmost solid curve in Fig. 3. It can be observed that the sequence of branches labelled $1, n$ exist for all values of β in $0 < \beta < \pi/2d$ whilst all other branches disappear through the

second cut-off illustrated in Fig. 4(a) by the dotted diagonal line before the value of $\beta = \pi/2d$ is reached. There is no obvious explanation for this behaviour.

A similar labelling technique is employed in Fig. 5(a and b) where the variation of kd and a/d with βd is again shown, but for blocks of widths $b/d = 0, 0.15, 0.3, 0.45$. For each value of b/d only two branches are sketched. They are labelled (1, 1) and (2, 1) which indicate that they are branches that originate from the first boxed values along the first two set of curves for Dirichlet trapped modes shown in Fig. 3. From Fig. 5(a) it can be seen that as b/d is increased the values of kd also increase whilst the interval of βd over which Rayleigh–Bloch solutions exist decreases. This is in accordance with the wide-spacing arguments of Section 4 which predicted that modes could only exist in the region $\pi/2c < k < \pi/d$ and for $0 < \beta d < \pi/d - \pi/2c$. Only the curve for $b/d = 0$ labelled 1, 1 has Rayleigh–Bloch solutions throughout the entire interval $0 < \beta < \pi/d - \pi/2c$, whilst all other curves disappear through the second cut-off before the limiting value of $\beta = \pi/d - \pi/2c$ is reached.

8. Rayleigh–Bloch waves above the second cut-off

The wide-spacing approximation at the end of Section 4 allowed us to argue the possibility of finding Rayleigh–Bloch waves whenever the number of wave-like modes between adjacent blocks is greater than in the region away from the blocks. Throughout the course of the present paper we have concentrated on the regime $\pi/2c < k < \pi/d - \beta$ for $0 < \beta < \pi/d - \pi/2c$ for which this is the case. In Fig. 2, this regime is represented by the triangular region of (k, β) space shaded grey and labelled with a bold (2, 1), lying above the first diagonal dashed line and below the second. The Rayleigh–Bloch solutions that we have found in this regime are, therefore, said to be above the first cut-off and below the second cut-off for the periodic array where the number of possible wave-like modes away from the array increases by one as k is increased across each cut-off.

When k is increased beyond the second cut-off we can consider the possibility of finding Rayleigh–Bloch waves in the regime $\pi/c < k < \pi/d + \beta$, $\pi/c - \pi/d < \beta < 3\pi/2d$ which only exists if $b < \frac{1}{3}d$. This region of (k, β) parameter space is represented by the hashed triangle labelled with a bold (3, 2) in Fig. 2 indicating that there are three possible wave-like modes between adjacent blocks in the array and two wave-like modes away from the array.

The motivation for seeking Rayleigh–Bloch modes above the second cut-off comes from the wide-spacing arguments of Section 4. These indicate that three conditions need to be satisfied which may be possible for the rectangular array, since the problem involves three independent parameters, kd, a/d and b/d.

It is a straightforward matter to adapt the integral equation formulation of Section 5 to consider possible Rayleigh–Bloch modes above the second cut-off. The outcome indeed turns out to be that *three* real conditions need to be satisfied for such a mode to exist, the first being the vanishing of the determinant of a real 3×3 symmetric matrix and the other two being supplementary conditions to ensure the amplitudes of modes in $x > 0$ (in this case B_0 and B_{-1}) are both zero.

In this case, the integral Eq. (5.7) applies now for $n = 0, 1, 2$ and with a slightly revised kernel,

$$K(y,t) = \sum_{n=-\infty}^{\infty}{}'' \frac{1}{2\gamma_n d}\Psi_n(y)\overline{\Psi_n(t)} + \sum_{n=3}^{\infty}\frac{\coth\alpha_n a}{2\alpha_n c}\psi_n(y)\overline{\psi_n(t)} \tag{8.1}$$

where the double dash indicates that the $n = 0$ and $n = -1$ terms are omitted from the infinite sum. Also note the second summation starts at $n = 3$. The integral operator $\mathcal{K}$ thus retains the properties it possessed in the working of Section 5. The solutions of the integral equations are used in (5.10) to give a real symmetric system of equations

$$\begin{pmatrix} S_{0,0} - 2k_0 c\tan k_0 a & S_{0,1} & S_{0,2} \\ S_{1,0} & S_{1,1} - 2k_1 c\tan k_1 a & S_{1,2} \\ S_{2,0} & S_{2,1} & S_{2,2} - 2k_2 c\tan k_2 a \end{pmatrix} \begin{pmatrix} \hat{A}_0 \\ \hat{A}_1 \\ \hat{A}_2 \end{pmatrix} = \begin{pmatrix} 0 \\ 0 \\ 0 \end{pmatrix} \tag{8.2}$$

In order for a Rayleigh–Bloch wave to exist the determinant of the 3×3 matrix, $\mathbf{S}$, above must vanish to yield non-trivial real coefficients $\hat{A}_n$, $n = 0, 1, 2$ which must then also simultaneously satisfy the *pair* of real side conditions

$$\left.\begin{aligned} 2\,\mathrm{i}\kappa_0 d B_0 &= \{\hat{A}_0 P_{0,0} + \hat{A}_1 P_{0,1} + \hat{A}_2 P_{0,2}\} = 0 \\ 2\,\mathrm{i}\kappa_{-1} d B_{-1} &= \{\hat{A}_0 P_{-1,0} + \hat{A}_1 P_{-1,1} + \hat{A}_2 P_{-1,2}\} = 0 \end{aligned}\right\} \tag{8.3}$$

with $P_{m,n}$ defined by (5.14) as before.

The solution of the integral equations and the values of $S_{m,n}$ and $P_{m,n}$ are determined using the Galerkin approximation employed in Section 6 with appropriate modifications. However, the numerical procedure used for locating Rayleigh–Bloch solutions is rather more complicated since three conditions need to be met simultaneously. Instead of identifying a solution as being the crossing of two curves in $(kd, a/d)$ space, it turns out that a solution above the second cut-off for some given value of β now corresponds to the intersection at a point of three surfaces drawn in $(kd, a/d, b/d)$ space on each of which one of the three conditions is met.

As in the case with Rayleigh–Bloch waves above the first cut-off the main difficulty that needs to be overcome is to ascertain where in parameter space one should start looking for a Rayleigh–Bloch solution numerically. To assist in this we use the results of McIver et al. [16] who have produced curves for Neumann trapped modes above the first cut-off for rectangular blocks. These Neumann trapped modes correspond here to $\beta = \pi/2d$ and for $\pi/c < k < 3\pi/2d$—an interval on Fig. 2 labelled with a rotated bold (2, 1). The significance of the results of McIver et al. [16] is that they are adjacent in (k, β) parameter space to the region in which we wish to seek Rayleigh–Bloch waves above the second cut-off. The curves in McIver et al. [16] are generated by simultaneously satisfying a *pair* of conditions, but once β is taken to have a value of less than $\pi/2d$ the satisfaction of *three* conditions are needed to produce a Rayleigh–Bloch solution.

The procedure we use is similar to that already described in detail for Rayleigh–Bloch waves above the first cut-off. We choose a value of $\beta = \pi/2d - \epsilon$ where ϵ is small and use the solutions generated in McIver et al. [16] to identify a starting point for a branch of Rayleigh–Bloch solutions by generating a similar set of curves that satisfy two of the three conditions, namely $\det(\mathbf{S}) = 0$ and $B_0 = 0$. Along each of these curves we monitor the value of B_{-1} and look for a change in sign indicating that B_{-1} has passed through zero along one of these curves. Where it passes through zero all three conditions are met simultaneously and we have, therefore, located numerically a Rayleigh–Bloch solution. In fact this only happens for a single set of values of $(kd, a/d, b/d)$ which are marked on Fig. 6 with a box. Fig. 6 repeats the curves in Figs. 2 and 3 of McIver et al. [16] showing embedded Neumann trapped

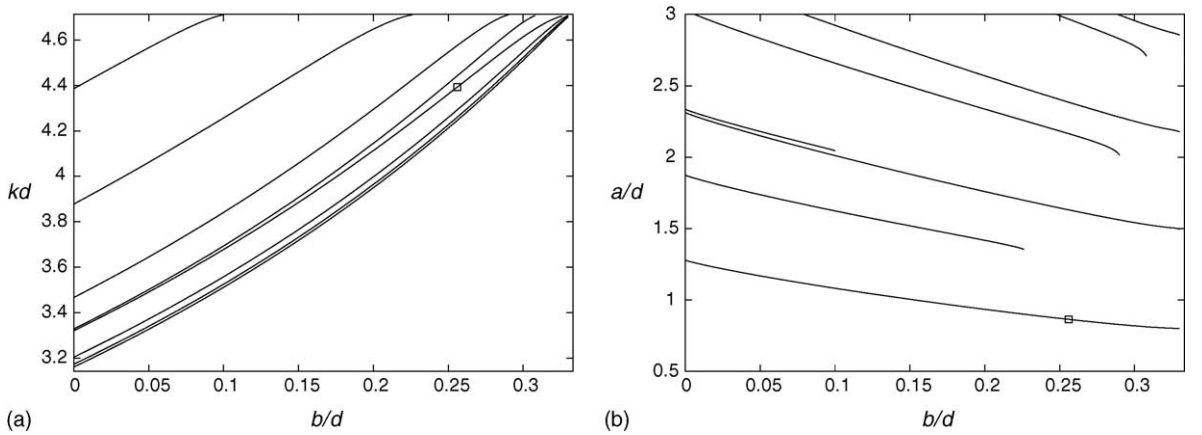

Fig. 6. Variation of (a) kd, (b) a/d with b/d for Neumann trapped modes (Rayleigh–Bloch waves with $\beta d = \pi/2$) above the first cut-off (see McIver et al. [16] for detailed labelling).

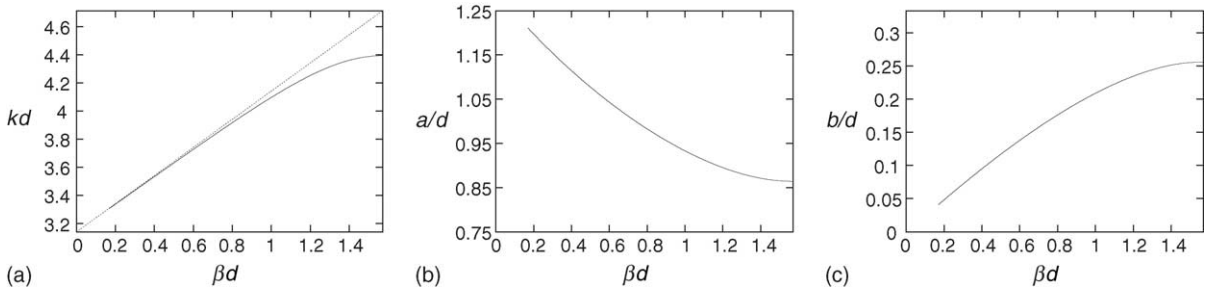

Fig. 7. Variation of (a) kd, (b) a/d and (c) b/d with βd for Rayleigh–Bloch waves above the second cut-off (dotted line).

wave parameters, by using the integral equation methods outlined in this paper. Once the set of values $(kd, a/d, b/d)$ have been found for $\beta = \pi/2d - \epsilon$ indicating the starting point of a branch into $\beta < \pi/2d$, the branch can be tracked for decreasing values of β to find how kd, a/d and b/d vary with β resulting in the set of three curves in Fig. 7(a–c). To the authors' knowledge these are the first examples of any form of embedded wave solution occurring above a second cut-off.

Although the procedure outlined above is sufficient to produce accurate numerical results, it may be argued that it is not a rigorous numerical proof of existence of Rayleigh–Bloch waves above the second cut-off, since in the procedure outlined above the value of B_{-1} is being evaluated using values on curves that are only approximate since they have been generated numerically. A stronger piece of evidence for the existence of Rayleigh–Bloch waves above the second cut-off is demonstrated in Fig. 8(a and b). Here, curves on which $\det(\mathbf{S}) = 0$, $\tilde{B}_0 = 0$ and $\tilde{B}_{-1} = 0$ are drawn in $(kd, a/d)$ space for two values of b/d. Here, as in Evans and Porter [8]), we have defined modified quantities $\tilde{B}_0$ and $\tilde{B}_{-1}$ which are defined away from the curve $\det(\mathbf{S}) = 0$ using coefficients $\hat{A}_n$, $n = 0, 1, 2$ that are defined to be the eigenvector of (8.2) generated by the smallest eigenvalue in modulus of the matrix $\mathbf{S}$. Whenever curves of either $\tilde{B}_0 = 0$ or $\tilde{B}_{-1} = 0$ cross the curve $\det(\mathbf{S}) = 0$ the smallest eigenvalue is clearly zero and therefore the values of $\tilde{B}_n$ coincide with B_n, $n = 0, -1$ at those points. The crucial point is that in Fig. 8(a and b) each of the three curves are generated *independently* of one another. Clearly in each figure both curves of $\tilde{B}_0 = 0$ and $\tilde{B}_{-1} = 0$ cross the curve $\det(\mathbf{S}) = 0$. The characteristic difference between Fig. 8(a and b) is that the order in which the two curves $\tilde{B}_0 = 0$ and $\tilde{B}_{-1} = 0$ intersect the curve $\det(\mathbf{S}) = 0$. Since the curves vary continuously as b/d is increased

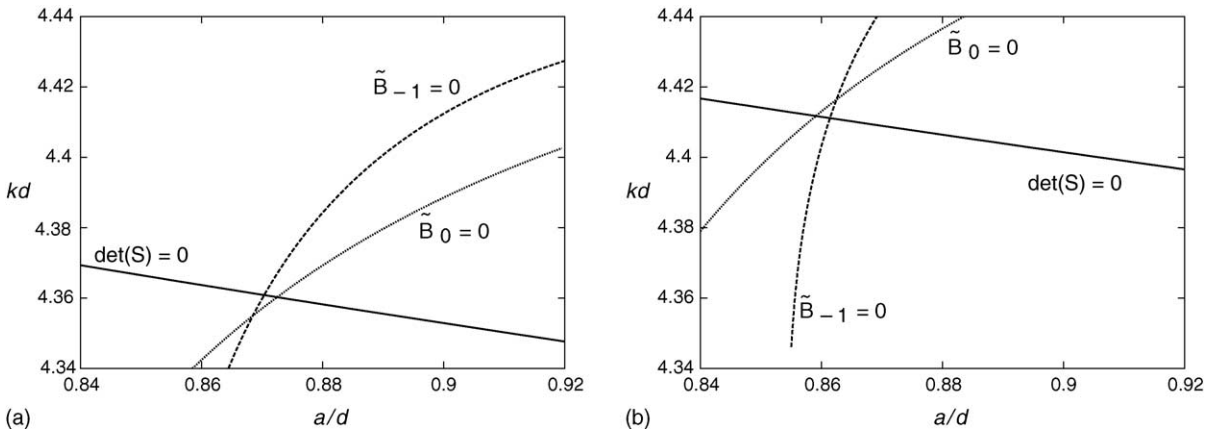

Fig. 8. Curves showing zeros of the three conditions that are required for a Rayleigh–Bloch solution above the second cut-off in the $(kd, a/d)$ plane for (a) $b/d = 0.25$ and (b) $b/d = 0.26$ when $\beta d = 1.5$.

from 0.25 in Fig. 8(a) to 0.26 in Fig. 8(b), there must be a value in the interval $b/d \in (0.25, 0.26)$ where all three curves intersect at a single point. Since the curves are computed independently, any small error introduced into the numerical solution of the integral equations will not alter the ordering of the crossing in the two figures and therefore the existence of a single crossing point is established.

9. Conclusions

Convincing numerical evidence for the existence of embedded Rayleigh–Bloch surface waves has been presented using an accurate Galerkin approximation to certain integral equations. Arguments for the existence of such modes was provided using a wide-spacing approach which illustrated the importance of the number of wave-like modes in each of two regions. Results for embedded Rayleigh–Bloch modes above the first cut-off indicate that for a given block width to spacing ratio satisfying $b/d < \frac{1}{2}$, for every β in $0 < \beta < \pi/2d$ there exists a Rayleigh–Bloch mode for discrete values of block length a/d with corresponding values of wavenumber k. This differs from results obtained for the same geometrical configuration by Evans and Fernyhough [5] who showed that below the cut-off Rayleigh–Bloch waves existed under the above conditions for *all* values of a/d. In going above the second cut-off, we have found that for each value of β in $0 < \beta_c < \beta < \pi/2d$ Rayleigh–Bloch modes exist for a single unique value of kd, a/d and b/d.

In each of these regimes, the scattering of an incident wave at an angle $\cos^{-1}(k/\beta)$ to the axis of the array would result in either one or two specularly reflected waves. At the parameter values corresponding to the Rayleigh–Bloch modes the scattering problem in each case becomes non-unique. It would be of interest to examine, for example, the variation of the reflection coefficients as the Rayleigh–Bloch mode solutions is approached through varying the angle of incidence for appropriate geometric parameters.

In the electromagnetic context Rayleigh–Bloch waves are described as slow, surface, or guided waves. See, for example, chapter 7 of Jones [11] where an approximate solution for the guided waves propagating along the outside of an axisymmetric corrugated rod is obtained. There is no reason why the methods described here for the two-dimensional periodic rectangular array should not carry over to give accurate results for the corrugated rod, including the prediction of the higher-order solutions above the first or second cut-off.

References

[1] M. Callan, C.M. Linton, D.V. Evans, Trapped modes in two-dimensional waveguides, J. Fluid Mech. 229 (1991) 51–64.
[2] R. Chaterjee, Elements of Microwave Engineering, Ellis-Horwood Limited, Chichester, 1983.
[3] E.B. Davies, L. Parnovski, Trapped modes in acoustic waveguides, Q. J. Mech. Appl. Maths. 51 (3) (1998) 477–492.
[4] R.S. Elliot, An Introduction to Guided Waves and Microwave Circuits, Prentice-Hall International, London, 1993.
[5] D.V. Evans, M. Fernyhough, Edge waves along periodic coastlines. Part 2, J. Fluid Mech. 297 (1995) 307–325.
[6] D.V. Evans, C.M. Linton, Edge waves along periodic coastlines, Q. J. Mech. Appl. Maths. 46 (1993) 644–656.
[7] D.V. Evans, C.M. Linton, Acoustic resonance in ducts, J. Sound. Vib. 173 (1994) 85–94.
[8] D.V. Evans, R. Porter, Trapped modes embedded in the continuous spectrum, Q. J. Mech. Appl. Math. 52 (1) (1998) 263–274.
[9] D.V. Evans, M. Levitin, D. Vassiliev, Existence theorems for trapped modes, J. Fluid Mech. 261 (1994) 21–31.
[10] M.D. Groves, Examples of embedded eigenvalues for problems in acoustic waveguides, Math. Methods Appl. Sci. 21 (6) (1998) 479–488.
[11] D.S. Jones, The Theory of Electromagnetism, Pergamon, Oxford, 1964.
[12] C.M. Linton, M. McIver, P. McIver, K. Ratcliffe, J. Zhang, Trapped modes for off-centre structures in guides, Wave Motion 36 (1) (2002) 67–85.
[13] H.D. Maniar, J.N. Newman, Wave diffraction by a long array of cylinders, J. Fluid Mech. 339 (1997) 309–330.
[14] M. McIver, C.M. Linton, On the non-existence or otherwise of trapped modes in acoustic waveguides, Q. J. Mech. Appl. Math. 43 (1995) 543–555.
[15] M. McIver, C.M. Linton, P. McIver, J. Zhang, R. Porter, Embedded trapped modes for obstacles in two-dimensional waveguides, Q. J. Mech. Appl. Math. 54 (2) (2001) 273–293.

[16] M. McIver, C.M. Linton, J. Zhang, The branch structure of embedded trapped modes in two-dimensional waveguides, Q. J. Mech. Appl. Maths 55 (2) (2002) 313–326.
[17] R. Porter, D.V. Evans, Rayleigh–Bloch surface waves along periodic gratings and their connection with trapped modes in channels, J. Fluid Mech. 386 (1999) 233–258.
[18] R. Porter, D. Porter, Interaction of water waves with three-dimensional periodic topography, J. Fluid Mech. 434 (2001) 301–335.
[19] T. Utsunomiya, R. Eatock-Taylor, Trapped modes around a row of circular cylinders in a channel, J. Fluid Mech. 386 (1999) 259–279.
[20] C.H. Wilcox, Scattering theory for diffraction gratings, Applied Mathematical Sciences, vol. 49, Springer, 1984.